



ORIGINAL ARTICLES

# Corrosion behaviour of thermal cycled aluminium hybrid composites reinforced with rice husk ash and silicon carbide



Kenneth Kanayo Alaneme\*, Joshua Ogheneakporobo Ekperusi, Samuel Ranti Oke

Department of Metallurgical and Materials Engineering, Federal University of Technology, Akure PMB 704, Nigeria

Received 30 August 2015; accepted 2 August 2016

Available online 9 August 2016

## KEYWORDS

Aluminium hybrid composites;  
Corrosion;  
Potentiodynamic electrochemical measurements;  
Rice husk ash;  
Structural stability;  
Thermal cycling

**Abstract** The corrosion behaviour of aluminium hybrid composites reinforced with rice husk ash and silicon carbide subjected to thermal cycling has been investigated. Aluminium hybrid composites having 10 wt% reinforcement consisting of silicon carbide (SiC) and rice husk ash (RHA) in weight ratios of 1:0, 3:1, 1:1, 1:3, and 0:1 respectively were produced. The composites were subjected to varying thermal cycles of 6, 12 and 18 from room temperature to 200 °C repeatedly. Potentiodynamic polarization measurements were used to study the corrosion behaviour of the produced composites. The results show that the composites displayed similar polarization curves and passivity characteristics irrespective of the number of thermal cycles both in H<sub>2</sub>SO<sub>4</sub> and NaCl solutions. No consistent trend of corrosion current density changes with increase in thermal cycling was established for composite grades 3:1, 1:1 in H<sub>2</sub>SO<sub>4</sub> and 1:0, 0:1 and 3:1 in NaCl solutions. The hybrid composite grades with a higher RHA content generally exhibited a lower tendency to corrode compared to the other composite grades. Generally, the composites seemed to be structurally stable as they maintained their corrosion resistance levels even after exposure to thermal cycling.

© 2016 The Authors. Production and hosting by Elsevier B.V. on behalf of King Saud University. This is an open access article under the CC BY-NC-ND license (<http://creativecommons.org/licenses/by-nc-nd/4.0/>).

## 1. Introduction

Aluminium matrix composites (AMCs) are a unique class of composite materials that are used for a wide range of applications. Their use pervades the aerospace, automotive, nuclear,

biotechnology, sports, recreational and thermal management applications (Asif et al., 2011; Alaneme and Bodunrin, 2013; Alaneme et al., 2014; Mohan et al., 2014; Suresha and Sridhara, 2010). Its attraction is mainly due to its low cost of processing, and wide spectrum of properties which include high specific strength, high specific stiffness, low thermal coefficient of expansion, improved tribological and corrosion properties (Ramachandra and Radhakrishna, 2005; Alaneme, 2011; Prasad et al., 2014).

AMCs have been used in the design of specific aerospace and automotive components such as ventral fins, fuel access door covers, rotating blade sleeves, gear parts, crankshafts, and suspension arms. In the electronic industry they are used in the

\* Corresponding author.

E-mail address: [kalanemek@yahoo.co.uk](mailto:kalanemek@yahoo.co.uk) (K.K. Alaneme).  
Peer review under responsibility of King Saud University.



processing of integrated heat sinks, microprocessor lids, microwave, aircraft wings, fuselage frames and landing gears (Macke et al., 2012; El-Labban et al., 2016). In most of these applications the components undergo cyclic thermal exposures due to the operational mechanism of the engineering systems of which they are part. (Mallik et al., 2011; Alaneme et al., 2015).

The increasing service performance expected from materials utilized for thermal management applications has buoyed interest in the development of advanced aluminium matrix composites (AMC) with high thermal conductivity (TC) to effectively dissipate heat and low coefficient of thermal expansion (CTE) to minimize thermal stresses (Qu et al., 2011; Requena et al., 2012). This is of vital importance to enhance the performance, life cycle and reliability of AMCs utilized in environments where they are exposed to intermittent or constant elevated temperatures (Chen et al., 2009). Indeed several works have been conducted on the thermal management capabilities of AMCs (Qu et al., 2011; Requena et al., 2012; Chen et al., 2009; Daguang et al., 2013; Huber et al., 2006) but sparse literatures are available for AMCs reinforced with agro waste ashes. Also the effect of repeated or fluctuating thermal cycles on the engineering properties of agro waste reinforced AMCs has rarely received attention.

It is instructive to note that ashes derived from controlled burning of agro wastes (such as coconut shell, rice husk, bamboo leaf, and bagasse among others) have been used as reinforcements in AMCs with very promising results obtained (Alaneme et al., 2018; Bodunrin et al., 2015; Alaneme et al., 2013; Alaneme and Olubambi, 2013). These agro waste ashes have advantages of low densities and processing cost compared with common synthetic reinforcing ceramics such as silicon carbide and alumina (Saravanan and Kumar, 2013).

In this research work, the effects of thermal cycling on the corrosion behaviour of Al based composites reinforced with rice husk ash and silicon carbide are investigated. The microstructural features of these composite grades have been reported by Alaneme and Adewale (2013); and the mechanical properties of the composites under the influence of thermal cycling have been reported to be stable (Alaneme et al., 2015; Ekperusi, 2016). However there is currently no available study which has considered the corrosion behaviour of these composites using potentiodynamic polarization technique as basis for electrochemical studies. This work is aimed at comparing the corrosion properties of low cost processed Al based composite grades with conventional reinforced AMCs in environments where they are liable to undergo thermal cycling.

## 2. Materials and methods

### 2.1. Materials

Al–Mg–Si alloy (Si: 0.40, Fe: 0.22, Cu: 0.01, Mn: 0.01, Mg: 0.40, Cr: 0.03, Zn: 0.02, Ti: 0.01, Ni: 0.01, Al: 98.88 in wt. %) was used as the metal matrix for this research. Chemically pure silicon carbide particles having average particle size of 28  $\mu\text{m}$  and rice husk ash were selected as hybrid reinforcements for the aluminium based composites to be produced.

### 2.2. Preparation of RHA

The rice husk ash was processed from rice husk following procedures reported in detail by Alaneme and Adewale, 2013. Rice husk ash was produced by burning rice husk completely with the aid of a metallic drum. The ash obtained from the process was conditioned in a furnace at a temperature of 650 °C for 180 min to reduce the volatile and carbonaceous constituents of the ash. Sieve size analysis was carried out on the conditioned ash using a digital sieve shaker. Particle sizes below 50  $\mu\text{m}$  were selected for use as reinforcement in the composites to be developed. The chemical composition of the rice husk ash in wt.% is: silica ( $\text{SiO}_2$ ): 91.59; carbon, C (4.8); calcium oxide, CaO (1.58); magnesium oxide, MgO (0.53); potassium oxide,  $\text{K}_2\text{O}$  (0.39); haematite, ( $\text{Fe}_2\text{O}_3$ ); sodium, Na, (trace), and titanium,  $\text{TiO}_2$  (0.20) (Alaneme et al., 2013).

### 2.3. Production of the Al based composites

Double stir casting process in accordance with Alaneme and Adewale, 2013 was adopted for the production of the composites. Charge calculation was used to determine the quantities of aluminium, rice husk ash (RHA) and silicon carbide (SiC) required to produce a hybrid composite of 10 wt% reinforcement consisting of RHA and SiC in weight ratios 0:1, 1:3, 1:1, 3:1, and 1:0. The rice husk ash and silicon carbide particles were initially preheated separately at a temperature of 250 °C to eliminate dampness and improve wettability with the molten Al–Mg–Si alloy. The Al ingots were charged into a gas-fired crucible furnace, and heated 30 °C above the liquidus temperature to ensure the alloy melts completely. The liquid alloy was then cooled in the furnace to a semi solid state at a temperature of about 600 °C. The preheated SiC and RHA were added at this temperature and stirring of the slurry was performed manually for 5 minutes. The composite slurry was then superheated to 720 °C and a second stirring process performed using a mechanical stirrer. The stirring operation was performed at a speed of 300 rpm for 10 min to help improve the distribution of the SiC and RHA particles in the aluminium based composite. The molten composite was then cast into prepared sand moulds inserted with metallic chills to increase the composite solidification rate.

### 2.4. Thermal cycling

The thermal cycling procedure adopted is in accordance with Alaneme et al., 2015. The as-cast composite materials were subjected to repeat heating and cooling cycles of 6, 12 and 18 cycles to a maximum temperature of 200 °C to room temperature (25 °C). Control samples of the composites which were not subjected to thermal cycling were also prepared for experimentation. The thermal cycling process was performed by heating the samples in an oven to 200 °C and held for 45 min before removal from the oven and cooled in air to complete a thermal cycle. This procedure was repeated for the respective number of thermal cycles desired.

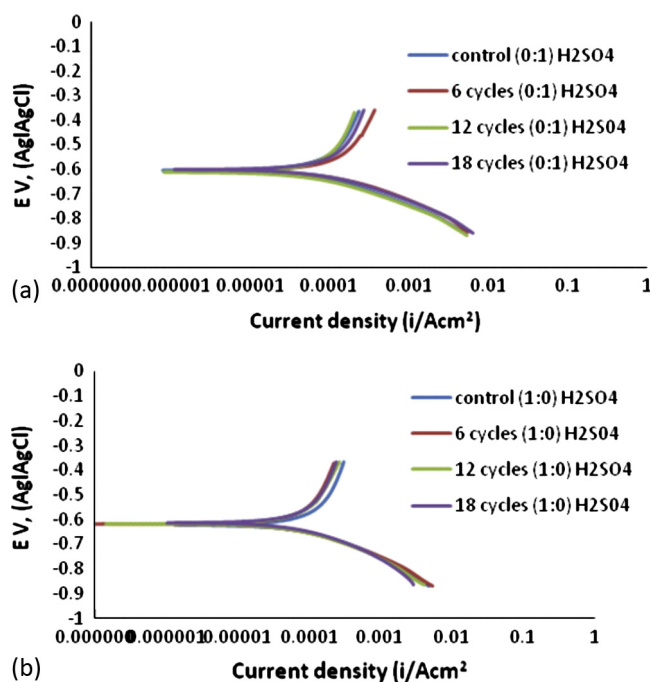


**Figure 1** Potentiodynamic polarization curves for (a) SiC reinforced aluminium composites, and (b) RHA reinforced aluminium composites; subjected to varied thermal cycles in 0.3 M H<sub>2</sub>SO<sub>4</sub> solution.

### 2.5. Corrosion test

Corrosion testing of the composites produced was conducted using potentiodynamic polarization electrochemical method. An AUTOLAB potentiostat was used as test facility for the corrosion experiment. All the corrosion tests were performed using a three-electrode corrosion cell set-up comprising the sample as the working electrode, saturated silver/silver chloride as reference electrode, and platinum as counter electrode. The working electrodes (composite samples) were prepared by attaching an insulated copper wire to one face of the sample using aluminium conducting tape, and cold mounting it in resin. The surfaces of the samples were wet ground with silicon carbide papers from 220 down to 600 grade in accordance with ASTM standard (ASTM G5-94, 2000), washed with distilled water, degreased with acetone and dried in air. Corrosion behaviour of the samples was investigated in 0.3 M H<sub>2</sub>SO<sub>4</sub> and 3.5%wt NaCl solution at room temperature (25 °C). Potentiodynamic polarization measurements were carried out using a scan rate of 1.0 mV/s at a potential initiated at -200 mV to +250 mV. After each experiment, the electrolyte was replaced, while the test samples were polished, rinsed in water and washed with acetone to remove the products that might have formed on the surface which could affect the measurement. Three repeat tests were carried out for all compositions of the composites, and the reproducibility and repeatability were observed to be good as there were no significant differences between results from triplicates.

**Table 1** Corrosion parameters from Potentiodynamic polarization curves for SiC reinforced aluminium, RHA reinforced aluminium, Al/1:1RHA-SiC, Al/1:3RHA-SiC, and Al/3:1RHA-SiC composites subjected to varied thermal cycles in 0.3 M H<sub>2</sub>SO<sub>4</sub> solution.

| Sample          | E <sub>corr</sub> /mV | I <sub>corr</sub> /Acm <sup>-2</sup> |
|-----------------|-----------------------|--------------------------------------|
| Control (0:1)   | -605                  | 1.74 × 10 <sup>-4</sup>              |
| 6 Cycles (0:1)  | -606                  | 1.60 × 10 <sup>-4</sup>              |
| 12 Cycles (0:1) | -612                  | 7.77 × 10 <sup>-5</sup>              |
| 18 Cycles (0:1) | -602                  | 1.20 × 10 <sup>-4</sup>              |
| Control (1:0)   | -622                  | 1.66 × 10 <sup>-4</sup>              |
| 6 Cycles (1:0)  | -618                  | 1.01 × 10 <sup>-4</sup>              |
| 12 Cycles (1:0) | -617                  | 5.58 × 10 <sup>-5</sup>              |
| 18 Cycles (1:0) | -612                  | 1.07 × 10 <sup>-4</sup>              |
| Control (1:3)   | -605                  | 1.56 × 10 <sup>-5</sup>              |
| 6 Cycles (1:3)  | -606                  | 3.67 × 10 <sup>-6</sup>              |
| 12 Cycles (1:3) | -612                  | 5.52 × 10 <sup>-7</sup>              |
| 18 Cycles (1:3) | -602                  | 9.17 × 10 <sup>-7</sup>              |
| Control (1:1)   | -744                  | 2.58 × 10 <sup>-6</sup>              |
| 6 Cycles (1:1)  | -729                  | 2.52 × 10 <sup>-6</sup>              |
| 12 Cycles (1:1) | -740                  | 2.34 × 10 <sup>-6</sup>              |
| 18 Cycles (1:1) | -765                  | 3.01 × 10 <sup>-5</sup>              |
| Control (3:1)   | -624                  | 6.10 × 10 <sup>-5</sup>              |
| 6 Cycles (3:1)  | -625                  | 4.46 × 10 <sup>-5</sup>              |
| 12 Cycles (3:1) | -612                  | 1.08 × 10 <sup>-4</sup>              |
| 18 Cycles (3:1) | -637                  | 6.13 × 10 <sup>-5</sup>              |

## 3. Results and discussion

### 3.1. Corrosion behaviour in 0.3M H<sub>2</sub>SO<sub>4</sub> solution

Fig. 1 shows the potentiodynamic polarization curves of the SiC and RHA single reinforced aluminium composites subjected to different thermal cycles and exposed to 0.3 M H<sub>2</sub>SO<sub>4</sub> solution. From Fig. 1(a) it is observed that all the SiC single reinforced aluminium composites displayed similar polarization trends and passivation characteristics. The electrochemical parameters, I<sub>corr</sub> and E<sub>corr</sub> values derived from the polarization plots are presented in Table 1. The table shows that the corrosion current density (I<sub>corr</sub>) of the single reinforced composites decreases with an increase in thermal cycles up to 12 cycles. This indicates that the sample subjected to 12 thermal cycles has the least kinetic tendency to corrode in 0.3 M H<sub>2</sub>SO<sub>4</sub> solution. Further thermal cycling to 18 cycles is observed to result in a slight increase in the I<sub>corr</sub> value relative to that of 12 cycles. It is noted that the I<sub>corr</sub> value for the sample subjected to 18 thermal cycles is less than that of the control sample which was not subjected to thermal cycling. This suggests that the thermal cycling does not deteriorate the corrosion resistance of the composite in 0.3 M H<sub>2</sub>SO<sub>4</sub> solution.

From Fig. 1(b), it is observed that the same polarization trends and passivation characteristics observed for the SiC reinforced composites (Fig. 1(a) and Table 1) is followed in the case of the RHA reinforced composites. Table 1 presents the electrochemical parameters associated with the general corrosion behaviour of the RHA reinforced aluminium composites in 0.3 M H<sub>2</sub>SO<sub>4</sub> solution. It is observed that the

composite sample subjected to 12 thermal cycles had the lowest  $I_{corr}$  value ( $5.58 \times 10^{-5} \text{ A/cm}^2$ ). This indicates it has the least susceptibility to corrosion in 0.3 M  $\text{H}_2\text{SO}_4$  solution compared to other composite grades. The  $I_{corr}$  value increases slightly when the thermal cycling is up to 18 cycles but the value is still not as high as that of the control sample (sample not subjected to thermal cycling). As in the case of the single reinforced aluminium – SiC composites, the corrosion tendency does not degrade below that of the control sample. This suggests that the samples are structurally stable and maintain their corrosion resistance levels even after exposure to thermal cycling.

The potentiodynamic polarization curves of the RHA–SiC hybrid reinforced aluminium composites subjected to thermal cycle in 0.3 M  $\text{H}_2\text{SO}_4$  are presented in Fig. 2. From Fig. 2(a) similar polarization curves and passivation tendency in the acidic medium are indicated. The results of the corrosion potentials and corrosion current densities obtained from the potentiodynamic polarization tests for the composites are summarized in Table 1. It is observed that the corrosion current densities of the composites decrease with an increase in thermal cycling up to 12 cycles. Further thermal cycling of the composites to 18 cycles resulted in a slight increase in the  $I_{corr}$  value but lower than that observed for the control and 6 thermal cycled samples. This is a good indicator that long term thermal cycling to a maximum temperature of 200 °C may not affect the corrosion resistance of the composites for the projected applications.

The potentiodynamic polarization curves of the reinforced aluminium (Al/1:1 RHA–SiC) subjected to thermal cycling and then exposed to  $\text{H}_2\text{SO}_4$  solution is presented in Fig. 2 (b). It is observed that hybrid reinforced composites exhibited similar polarization curves of direct passivation after the initial active corrosion where increase in corrosion current was proportional to applied potential. The shape of the polarization curves however differs slightly from that of both single reinforced composite grades considered earlier. The corrosion current density obtained from the polarization curves for the composites revealed relatively wide differences in the corrosion resistance. The  $I_{corr}$  and  $E_{corr}$  values (Table 1) did not suggest any definite corrosion pattern with an increase in thermal cycling as the composite without thermal cycling had relatively superior corrosion resistance to the 6 and 12 thermal cycled samples. Nonetheless, the least corrosion rate was obtained from the composite sample subjected to 18 thermal cycles which had the lowest corrosion current density value ( $5.67 \times 10^{-5} \text{ A/cm}^2$ ). The suppositions from the  $I_{corr}$  values are supported by the  $E_{corr}$  values as it can be seen that the samples subjected to 18 thermal cycles had the highest  $E_{corr}$  value followed by the control sample which suggests a less thermodynamic tendency to corrode in the 0.3 M  $\text{H}_2\text{SO}_4$  solution.

The potentiodynamic polarization curves of the RHA–SiC (3:1) hybrid reinforced aluminium composites subjected to different thermal cycling in 0.3 M  $\text{H}_2\text{SO}_4$  solution is presented in Fig. 2(c). It is observed that all the composite grades generally displayed similar polarization curve patterns and passivity characteristics. The electrochemical parameters associated with the general corrosion behaviour of the composites are summarized in Table 1. It is observed that no consistent trend of corrosion current density with an increase in thermal cycling could be established for these grades of composites. The  $E_{corr}$  values were not in tandem with the observations from the  $I_{corr}$

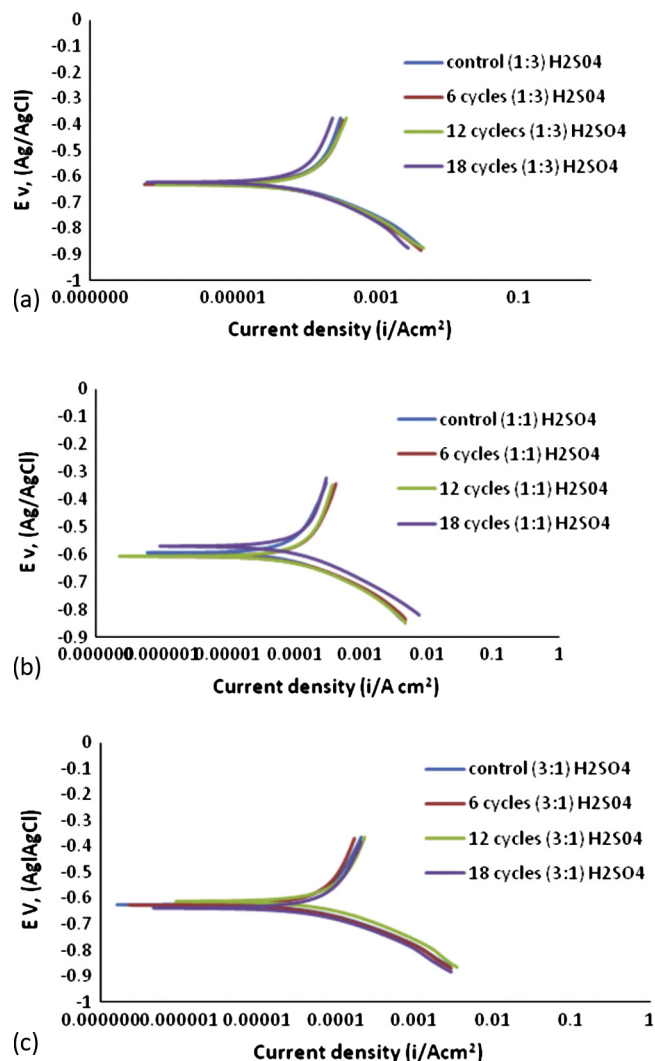


**Figure 2** Potentiodynamic polarization curves for (a) hybrid reinforced Al/RHA–SiC (1:3) composites, (b) hybrid reinforced Al/RHA–SiC (1:1) composites, and (c) hybrid reinforced Al/RHA–SiC (3:1) composites; subjected to varied thermal cycles in 0.3 M  $\text{H}_2\text{SO}_4$  solution.

and thus a conclusive position cannot be established for this composite series. Nonetheless, the least  $I_{corr}$  value ( $4.46 \times 10^{-5}$ ) and highest  $E_{corr}$  value ( $-612 \text{ mV}$ ) were obtained for the sample subjected to 6 thermal cycles from 200 °C. This indicates that the sample had the least tendency to corrode both from thermodynamics and kinetics considerations.

From Table 1, the electrochemical parameters ( $I_{corr}$  and  $E_{corr}$  values) of the composites which did not undergo thermal cycling can also be compared. It is observed that the composite grade containing RHA–SiC mix ratio of 3:1 has the least  $I_{corr}$  value indicating a lower susceptibility to corrosion in 0.3 M  $\text{H}_2\text{SO}_4$  solution. It is also noted that the hybrid composite grades with a higher RHA content (3:1 and 1:1) generally exhibited a lower tendency to corrode compared to the other composite grades.

### 3.2. Corrosion behaviour in 3.5% NaCl solution

Fig. 3 shows the potentiodynamic polarization curves of the SiC and RHA single reinforced aluminium composites subjected to different thermal cycles before exposure to 3.5% NaCl solution. It is observed from Fig. 3(a) that the SiC single reinforced aluminium composites displayed similar polarization curves and passivity characteristics. The corrosion current density obtained from the polarization curves for the composites revealed sufficient variation in the corrosion resistance. The  $I_{corr}$  and  $E_{corr}$  values (Table 2) show that there was no definite pattern or correlation between the corrosion rate and the number of thermal cycles. It is however noted that the samples subjected to 6 and 12 thermal cycles had the least  $I_{corr}$  values suggesting they have a lower tendency to corrode in NaCl solution in comparison with the other samples in this series from a kinetics appraisal.

For the RHA reinforced aluminium composite grades subjected to different thermal cycles and immersed in 3.5 wt.% of NaCl (Fig. 3b), similar trends in the polarization curve and passivity characteristics are apparent. The corrosion potential ( $E_{corr}$ ) and corrosion current density ( $I_{corr}$ ) data for the above grade of composites are presented in Table 2. It is observed that the single reinforced composite samples exposed to 18 thermal cycles had the least corrosion current densities compared to the 0, 6 and 12 thermal cycle samples. There was however no consistent trend of corrosion susceptibility

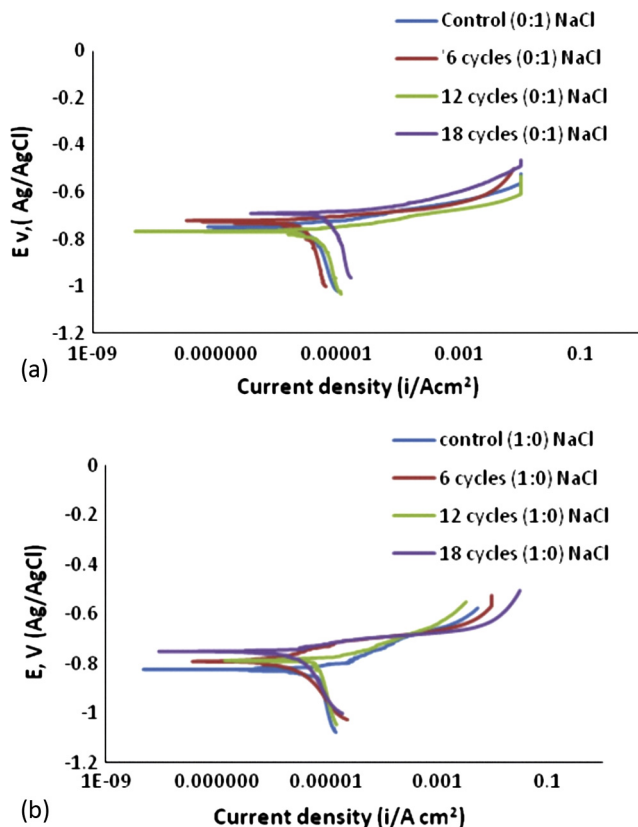


**Figure 3** Potentiodynamic polarization curves for (a) SiC reinforced aluminium composites, and (b) RHA reinforced aluminium composites; subjected to varied thermal cycles in 3.5 wt% NaCl solution.

**Table 2** Corrosion parameters from Potentiodynamic polarization curves for SiC reinforced aluminium, RHA reinforced aluminium, Al/1:1RHA–SiC, Al/1:3RHA–SiC, and Al/3:1RHA–SiC composites subjected to varied thermal cycles in 3.5wt% NaCl solution.

| Sample          | $E_{corr}/mV$ | $I_{corr}/Acm^{-2}$   |
|-----------------|---------------|-----------------------|
| Control (0:1)   | -751          | $2.67 \times 10^{-6}$ |
| 6 Cycles (0:1)  | -725          | $1.50 \times 10^{-6}$ |
| 12 Cycles (0:1) | -768          | $2.32 \times 10^{-6}$ |
| 18 Cycles (0:1) | -690          | $5.48 \times 10^{-6}$ |
| Control (1:0)   | -829          | $2.03 \times 10^{-6}$ |
| 6 Cycles (1:0)  | -793          | $1.48 \times 10^{-6}$ |
| 12 Cycles (1:0) | -791          | $1.98 \times 10^{-5}$ |
| 18 Cycles (1:0) | -685          | $4.93 \times 10^{-6}$ |
| Control (1:3)   | -605          | $1.56 \times 10^{-5}$ |
| 6 Cycles (1:3)  | -606          | $3.67 \times 10^{-6}$ |
| 12 Cycles (1:3) | -612          | $5.52 \times 10^{-7}$ |
| 18 Cycles (1:3) | -602          | $9.17 \times 10^{-7}$ |
| Control (1:1)   | -744          | $2.58 \times 10^{-6}$ |
| 6 Cycles (1:1)  | -729          | $2.52 \times 10^{-6}$ |
| 12 Cycles (1:1) | -740          | $2.34 \times 10^{-6}$ |
| 18 Cycles (1:1) | -765          | $3.01 \times 10^{-5}$ |
| Control (3:1)   | -752          | $7.31 \times 10^{-6}$ |
| 6 Cycles (3:1)  | -768          | $2.67 \times 10^{-6}$ |
| 12 Cycles (3:1) | -707          | $7.03 \times 10^{-6}$ |
| 18 Cycles (3:1) | -753          | $4.93 \times 10^{-6}$ |

with an increase or decrease in thermal cycles. The  $E_{corr}$  value for the 18 thermal cycles sample is observed to be the highest confirming that both from a thermodynamic and kinetic considerations the sample with 18 thermal cycles had the least susceptibility to corrosion in 3.5% NaCl solution.

The potentiodynamic polarization curves for the RHA–SiC hybrid reinforced Al composites in 3.5% NaCl solution (Fig. 4) provide information on the corrosion behaviour of the composites. From Fig. 4(a), it is observed that the RHA: SiC (weight ratio 1:3) hybrid reinforced composites irrespective of the number of thermal cycles generally displayed similar polarization curves and passivity characteristics. The results for the corrosion potentials ( $E_{corr}$ ) and corrosion current densities ( $I_{corr}$ ) for the composites are summarized in Table 2. It is observed from the data that the composites subjected to higher degree of thermal cycling appeared to be more resistant to corrosion. The resistance to corrosion is observed to be highest in the sample subjected to 12 cycles, which has the lowest  $I_{corr}$  value. Thermal cycling to 18 cycles resulted in a slight increase in the  $I_{corr}$  value relative to that of 12 cycles; but the corrosion rate was lower than that for the control and 6 thermal cycled samples.

The potentiodynamic polarization curves for the RHA–SiC (weight ratio 1:1) hybrid reinforced Al composites in 3.5% NaCl solution are presented in Fig. 4(b). It is observed that the composites displayed similar polarization curves and passivity characteristics. However, Table 2 which presents the corrosion potential ( $E_{corr}$ ) and corrosion current density ( $I_{corr}$ ) data, shows clearly that the corrosion current density ( $I_{corr}$ ) decreases with an increase in thermal cycling up to 12 cycles.

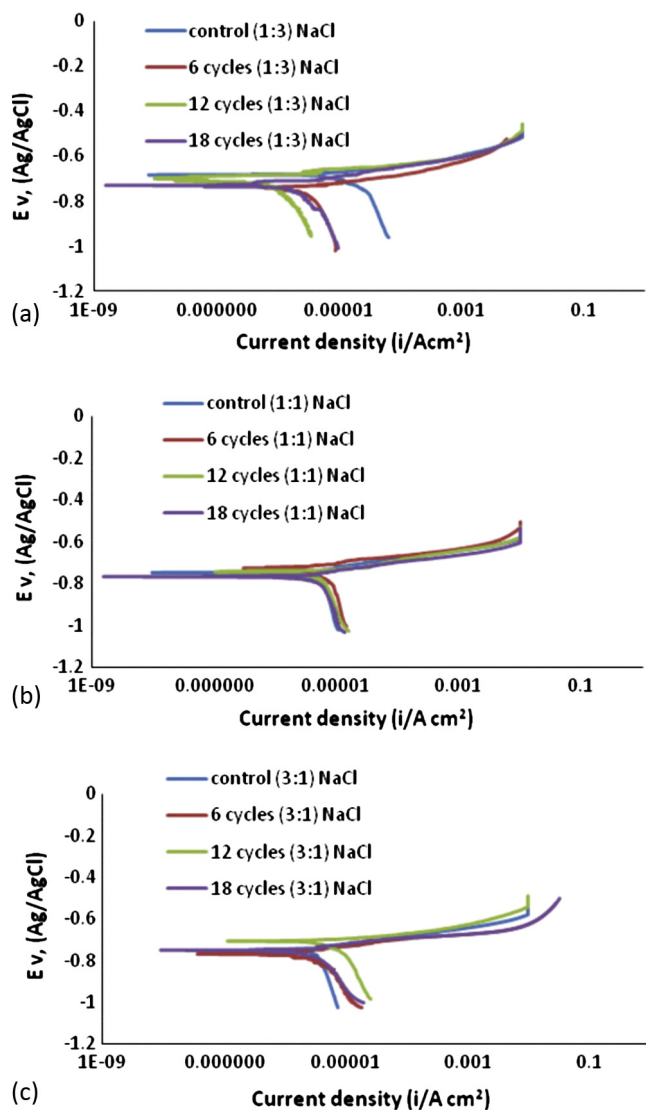


**Figure 4** Potentiodynamic polarization curves for (a) hybrid reinforced Al/RHA-SiC (1:3) composites, (b) hybrid reinforced Al/RHA-SiC (1:1) composites, and (c) hybrid reinforced Al/RHA-SiC (3:1) composites; subjected to varied thermal cycles in 3.5 wt% NaCl solution.

This signifies that the kinetic tendency to corrode of the composites decreases with increasing thermal cycling up to 12 cycles. Increasing the number of thermal cycles beyond 12 cycles to 18 cycles made the composite more susceptible to corrosion by increasing the corrosion current above that of the other three composite grades. From the  $E_{corr}$  values it is observed that the composite subjected to 18 cycles has the least  $E_{corr}$  value thus having the most thermodynamic tendency to corrode.

The potentiodynamic polarization curves of the RHA-SiC (weight ratio 3:1) hybrid reinforced aluminium matrix composites subjected to thermal cycling and exposed to 3.5 wt% NaCl solution are presented in Fig. 4(c). It is observed that the composites show slightly distinct polarization curves and passivity characteristics. The  $I_{corr}$  and  $E_{corr}$  values presented in Table 2 show that the corrosion behaviour of the composites did not

follow a consistent pattern. However, it is noted that the control sample has the highest  $I_{corr}$  value which indicates a higher kinetic tendency to corrode in 3.5% NaCl solution compared with the thermal cycled samples. This also demonstrates that thermal cycling of the hybrid composites did not result in increased susceptibility to corrosion of the composites.

From Table 2 it is also clearly seen that the corrosion potentials ( $E_{corr}$ ) and corrosion current density ( $I_{corr}$ ) of the composites which did not undergo thermal cycling did not follow a consistent trend. The composite compositions containing RHA (with the exception of the hybrid composition of RHA:SiC of 3:1) had lower  $I_{corr}$  values in comparison to the unreinforced and the SiC single reinforced aluminium matrix composite. This affirms that the use of the agrowaste derived RHA improves the corrosion resistance of the aluminium based composites.

#### 4. Conclusion

The corrosion behaviour of aluminium hybrid composites reinforced with rice husk ash and silicon carbide subjected to thermal cycling was investigated. From the results, the following conclusions are drawn:

- The composites displayed similar polarization curves and passivity characteristics, irrespective of the number of thermal cycles both in H<sub>2</sub>SO<sub>4</sub> and NaCl.
- No consistent trend of corrosion current density changes with an increase in thermal cycling was established for composites grades 3:1, 1:1 in H<sub>2</sub>SO<sub>4</sub> and 1:0, 0:1 and 3:1 in NaCl solutions.
- The hybrid composite grades with a higher RHA content generally exhibited a lower tendency to corrode compared to the other composite grades.
- Generally, the composites are structurally stable and maintain their corrosion resistance levels even after exposure to thermal cycling.

#### References

- Alaneme, K.K., 2011. Corrosion behaviour of heat-treated Al-6063/SiCp composites immersed in 5 wt% NaCl solution. *Leonardo J. Sci.* 18, 55–64.
- Alaneme, K.K., Adewale, T.M., 2013. Influence of rice husk ash/silicon carbide weight ratios on the mechanical behaviour of aluminium matrix hybrid composites. *Tribol. Ind.* 35, 163–172.
- Alaneme, K.K., Bodunrin, M.O., 2013. Mechanical behaviour of alumina reinforced AA (6063) metal matrix composites developed by two – step stir casting process. *Acta Tech. Corv. – Bull. Eng. Fascicule 3*, 105–110.
- Alaneme, K.K., Olubambi, P.A., 2013. Corrosion and wear behaviour of rice husk ash–alumina reinforced Al–Mg–Si alloy matrix hybrid composites. *J. Mater. Res. Technol.* 2, 188–194.
- Alaneme, K.K., Akintunde, I.B., Olubambi, P.A., Adewale, T.M., 2013. Mechanical behaviour of rice husk ash–alumina hybrid reinforced aluminium based matrix composites. *J. Mater. Res. Technol.* 2, 60–67.
- Alaneme, K.K., Olubambi, P.A., Afolabi, A.S., Bodunrin, M.O., 2014. Corrosion and tribological studies of bamboo leaf ash and alumina reinforced Al–Mg–Si alloy matrix hybrid composites in chloride medium. *Int. J. Electrochem. Sci.* 9, 5663–5674.

- Alaneme, K.K., Anabaranze, Y.O., Oke, S.R., 2015. Softening resistance, dimensional stability and corrosion behaviour of alumina and rice husk ash reinforced aluminium matrix composites subjected to thermal cycling. *Tribol. Ind.* 37, 204–214.
- Alaneme, K.K., Bodunrin, M.O., Awe, A.A., 2018. Microstructure, mechanical and fracture properties of groundnut shell ash and silicon carbide dispersion strengthened aluminium matrix composites. *J. King Saud Univ. – Eng. Sci.* 30 (1), 96–103.
- Asif, M., Chandra, K., Misra, P.S., 2011. Development of aluminium based hybrid metal matrix composites for heavy duty applications. *J. Miner. Mater. Charact. Eng.* 10, 1337–1344.
- ASTM G5–94, 2000. Annual book of ASTM standards, standard reference test method for making potentiostatic and potentiodynamic anodic polarization, measurements. 3, 57–67.
- Bodunrin, M.O., Alaneme, K.K., Chown, L.H., 2015. Aluminium matrix hybrid composites: a review of reinforcement philosophies; mechanical, corrosion and tribological characteristics. *J. Mater. Res. Technol.* 4 (4), 434–445.
- Chen, N., Zhang, H., Gu, M., Jin, Y., 2009. Effect of thermal cycling on the expansion behavior of Al/SiCp composite. *J. Mater. Proc. Technol.* 209, 1471–1476.
- Daguang, L., Guoqin, C., Longtao, J., Ziyang, X., Yunhe, Z., Gaohui, W., 2013. Effect of thermal cycling on the mechanical properties of Cf/Al composites. *Mater. Sci. Eng. A* 586, 330–337.
- Ekperusi, J.O., 2016. Softening resistance and corrosion behaviour of aluminium matrix composites reinforced with silicon carbide and rice husk ash (M.Eng thesis). Federal University of Technology, Akure, Nigeria.
- El-Labban, H.F., Abdelaziz, M., Mahmoud, E.R.I., 2016. Preparation and characterization of squeeze cast-Al-Si piston alloy reinforced by Ni and nano- $\text{Al}_2\text{O}_3$  particles. *J. King Saud Univ. – Eng. Sci.* 28 (2), 230–239.
- Huber, T., Degischer, H.P., Lefranc, G., Schmitt, T., 2006. Thermal expansion studies of aluminum-matrix composites with different reinforced architecture of SiC particles. *Comp. Sci. Technol.* 66, 2206–2217.
- Macke, A., Schultz, B.F., Rohatgi, P., 2012. Metal matrix composites offer the automotive industry an opportunity to reduce vehicle weight, improve performance. *Adv. Mater. Proc.* 170, 19–23.
- Mallik, S., Ekere, N., Best, C., Bhatti, R., 2011. Investigation of thermal management materials for automotive electronic control units. *Appl. Therm. Eng.* 31, 355–362.
- Mohan Krishna, S.A., Shridhar, T.N., Krishnamurthy, L., 2014. An investigative review on thermal characterization of hybrid metal matrix composites. *Int. J. Mod. Eng. Res.* 4, 53–62.
- Prasad, D.S., Shoba, C., Ramanaiah, N., 2014. Investigations on mechanical properties of aluminum hybrid composites. *J. Mater. Res. Technol.* 3, 79–85.
- Qu, X., Zhang, L., Wu, M., Ren, S., 2011. Review of metal matrix composites with high thermal conductivity for thermal management applications. *Prog. Nat. Sci. Mater. Int.* 21, 189–197.
- Ramachandra, M., Radhakrishna, K., 2005. Synthesis-microstructure-mechanical properties-wear and corrosion behavior of an Al-Si (12%) – flyash metal matrix composite. *J. Mater. Sci.* 40, 5989–5997.
- Requena, G., Yubero, D.C., Corrochano, J., Repper, J., Garcés, G., 2012. Stress relaxation during thermal cycling of particle reinforced aluminium matrix composites. *Comp. Part A Appl. Sci. Manuf.* 43, 1981–1988.
- Saravanan, S.D., kumar, M.S., 2013. Effect of mechanical properties on rice husk ash reinforced aluminum alloy (AlSi10Mg) matrix composites. *Proc. Eng.* 64, 1505–1513.
- Suresha, S., Sridhara, B.K., 2010. Wear characteristics of hybrid aluminium matrix composites reinforced with graphite and silicon carbide particulates. *Comp. Sci. Technol.* 70, 1652–1659.